Doppler Spread in Reverberation Chamber Predicted From Measurements During Step-Wise Stationary Stirring

Kristian Karlsson, Xiaoming Chen, Per-Simon Kildal, *Fellow, IEEE*, and Jan Carlsson, *Member, IEEE*

***Abstract*—We propose a simple method to accurately predict Doppler spread in a reverberation chamber (RC) by using frequency domain S-parameters measured with a vector network analyzer (VNA) at many fixed stirrer positions (step-wise stationary mode). Thus, the measurements are done under repeatable *stationary* conditions, so no Doppler shift is present during the actual measurements. Still, this letter shows that the measured S-parameters in step-wise stationary mode can be used to determine Doppler spread appearing during continuous movement of the stirrers. This can be done by computation for any stirrer speed by assuming that the fixed stirrer position steps are the time steps of a continuous movement of the stirrers, and by adding a virtual stirrer speed between the positions corresponding to the desired continuous movement of the stirrers. The computed Doppler spreads are validated over a large frequency band by measuring the time-varying S-parameters for a given stirrer speed.**

***Index Terms*—Channel transfer function, Doppler spread, reverberation chamber.**

I. Introduction

REVERBERATION chambers (RCs) were traditionally used for electromagnetic compatibility (EMC) measurements, but during the past decade they have found new applications for measuring over-the-air (OTA) performance of small antenna and wireless devices in multipath environment. The RC is basically a metal cavity, which is stirred to emulate a Rayleigh fading environment [1]. It has been used to measure antenna radiation efficiency, diversity gains, and capacity of multiple-input–multiple-output (MIMO) systems [2]. It can also be used to measure total radiated power [3] and total isotropic sensitivity [4] of active wireless devices and stations. The latter quantity may be affected by the delay spread, coherence bandwidth, Doppler spread, and coherence time of the propagation channels in the RC. Therefore, it is of importance to characterize these channel parameters. While the first two have been studied in [5], the main purpose of this letter is to characterize Doppler spread in RC (with coherence time being inversely proportional to it [6].

There is strong interest in estimating Doppler spread in wireless communications; and different methods have been studied [7]–[9]. While [7] and [8] deal with direct evaluation from the formula defining Doppler spread, [9] is mainly dealing with Doppler spread estimation in the presence of carrier frequency offset (CFO). By doing channel sounding in RC with a vector network analyzer (VNA), CFO problem is avoided, and therefore we do not need to resort to sophisticated signal processing algorithm as shown in [9]. Doppler spread in RC has previously been observed by simply sweeping intermediate frequency (IF) bandwidth of the VNA in continuous wave mode and observing the power variation [10]. However, this method gives only a rough estimation of Doppler frequency, and it works for only one single frequency at the time. Instead, we will show how the Doppler spread can easily be obtained for assumed stirrer speed even though the measurements themselves are done when the stirrers are stationary. Thus, each VNA measurement is done under stationary conditions with no Doppler shift. The theory behind this approach will be presented. The advantage of the step-wise stationary method is, in addition to the simplicity of the measurement setup, that we can obtain Doppler spread with very small computational effort, from S-parameters measured under stationary conditions, as a function of frequency for any enforced stirrer speed. This method is validated by actual measurements of Doppler spread in time domain in continuous stirring mode for a specific stirrer speed.

II. Doppler Spread

A. Derivation of Doppler Spread

We denote the channel transfer function $H(f,t)$. Then, its time autocorrelation function is

$$R_H(f,\partial t) = E[H^*(f,t)H(f,t+\partial t)] \tag{1}$$

where E represents mathematical expectation. If we now denote ρ the Doppler frequency, the Doppler spectrum becomes [7]

$$D(f,\rho) = \int_{-\infty}^{\infty} R_H(f,\partial t)\exp(-j2\pi\rho\partial t)d(\partial t). \tag{2}$$

Doppler spread B_D is defined as the range of Doppler frequency ρ over which $D(f,\rho)$ is above a certain threshold [7],

Manuscript received April 23, 2010; accepted May 18, 2010. Date of publication May 27, 2010; date of current version June 07, 2010. This work was supported in part by the Swedish Governmental Agency for Innovation Systems (VINNOVA) within the VINN Excellence Center Chase and by the Swedish Foundation for Strategic Research (SSF) within the Strategic Research Center Charmant.

K. Karlsson is with the Electronics Department, Technical Research Institute of Sweden, 501 15 Boras, Sweden (e-mail: kristian.karlsson@sp.se).

X. Chen, P.-S. Kildal, and J. Carlsson are with Antenna Group, Chalmers University of Technology, 412 96 Gothenburg, Sweden (e-mail: xiaoming.chen@chalmers.se).

Color versions of one or more of the figures in this letter are available online at http://ieeexplore.ieee.org.

Digital Object Identifier 10.1109/LAWP.2010.2051211

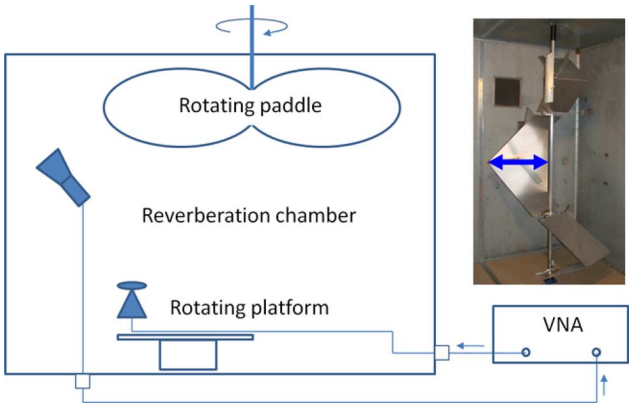

Fig. 1. Illustration of measurement setup with rotating paddle and platform. The actual mechanical stirrers used in the measurements are shown in photo with its maximum radius specified by the arrow.

[8]. Note that with $R_H(f,\partial t)$ being complex-conjugate symmetric, its Fourier transform $D(f,\rho)$ is real.

The autocorrelation function (1) is equivalent to

$$R_H(f,\partial t) = H(f,\partial t) \otimes H^*(f,-\partial t) \tag{3}$$

where $\otimes$ represents convolution. Applying Fourier transform to both sides of (3), we easily obtain [8]

$$D(f,\rho) = H(f,\rho)H^*(f,\rho) = |H(f,\rho)|^2 \tag{4}$$

where $H(f,\rho)$ is the Fourier transform of $H(f,t)$ w.r.t. time t, and the superscript * represents complex conjugation.

We will now explain why (4) is much easier to evaluate than (2). The channel transfer function $H(f,t)$ is equal to the S-parameter $S_{21}(f,t)$ measured with a VNA under stationary conditions, i.e., when the stirrers are fixed, corresponding to constant time t along the fading time scale. Such stationary measurements can then be repeated for many different time moments t_n, corresponding to different fixed stirrer positions s_n, with $n = 1,\dots N$ for the different stirrer positions. Although each of these S-parameters are measured under stationary conditions without Doppler shift, we can readily obtain the time varying S-parameter $S_{21}(f,t)$ for a given stirrer speed v by linking the discrete samples $S_{21}(f,t_n)$ using $t_n = t_{n-1} + (s_n - s_{n-1})/v$. Using this time-versus-stirrer-speed relation, the discrete Fourier transform of $H(f,t_n) = S_{21}(f,t_n)$ can readily be evaluated as explained below, and then finally Doppler spectrum is obtained using (4).

III. Measurements and Results

The RC used in this letter is located at SP Technical Research Institute of Sweden (SP), Boras, Sweden, which during these measurements makes use of rotating paddle and platform stirring; see Fig. 1. The transmitting antenna is a Discone antenna mounted on the platform, and the receiving antenna is a horn directed into a corner of the chamber. The size of the SP RC is: length 3 m, width 2.45 m, and height 2.45 m.

As explained, Doppler power spectrum present in an RC can be found by first measuring the channel transfer function $H(f,t_n)$ for all fixed stirrer positions n. The data can most conveniently be collected by measuring frequency sweeps with a VNA for each stirrer position, i.e., like a normal calibration measurement. To get a correct estimate of Doppler power spectrum, the spatial distance between the stirrer positions should be small enough to satisfy Nyquist theorem. This is in contradiction to a normal RC measurement where the step size shall be large enough to provide uncorrelated samples.

When $H(f,t_n)$ has been measured for all stirrer positions, Doppler power spectrum can be calculated using (4).

The discrete Doppler power spectrum will now have a frequency axis ranging from 0 to $N-1$. To convert this into a Doppler frequency domain, one can imagine the mode-stirrer running continuously through all the positions. With a time step Δt between the measured samples, the total time for one revolution will be $N\Delta t$, and sampling theory will give us a frequency axis in the interval $\rho \in [-\rho_{\max},\ \rho_{\max}]$, where $\rho_{\max}$ and the frequency step $\Delta\rho$ between each Doppler frequency sample can be expressed as

$$\rho_{\max} = \frac{1}{2\Delta t};\quad \Delta\rho = \frac{\rho_{\max}}{N} = \frac{1}{2N\Delta t}. \tag{5}$$

Each discrete frequency is given by $\rho_i = i\Delta\rho; i = -N, -(N-1),\dots,-1,0,1,\dots(N-1),N$.

A predicted spectrum for a test with "continuously" moving stirrers is shown in Fig. 2. For this measurement, a stirring sequence was defined as the rotation of one paddle 360°, and this was divided into $N = 720$ steps, giving a step size of 0.5°. Total time for one revolution during the test was set to 20 s, resulting in $\Delta t = 20/720$ s and $\rho_{\max} = 18$ Hz.

The following measurement procedure can now be performed to determine revolution time of the stirrer sequence in order to achieve a certain desired Doppler spread.

1. Define a stirring sequence that shall be used for generation of a Doppler environment for testing a device under test (DUT).
2. Step-wise move though the stirrer sequence with small enough steps (correlated data), and measure $S_{21}(f,t_n)$ at each stirrer position s_n with a VNA.
3. Use all $S_{21}(f,t_n)$ to calculate the Doppler power spectrum at all frequency points using (4).
4. Determine the desired Doppler frequency point $i = i_{\mathrm{D}}$ according to certain threshold in the calculated Doppler spectrum.
5. Establish the required revolution time of the stirrer sequence (or the corresponding stirrer speed) to obtain a desired chosen Doppler shift ρ_{D} from $T = N\Delta t = 1/2\Delta\rho = i_{\mathrm{D}}/2\rho_{\mathrm{D}}$.
6. Use continuous stirring to produce actual desired Doppler spread for DUT with the speed determined in step 5.

Instead of selecting a threshold for determining the Doppler spread, the RMS Doppler bandwidth can be used, which avoids the ambiguities introduced by different thresholds [7], [8]. The RMS Doppler bandwidth at a certain frequency f_0 is given by

$$\rho_{\mathrm{rms}} = \left[\frac{\int \rho^2 D(f_0,\rho)\,d\rho}{\int D(f_0,\rho)\,d\rho}\right]^{1/2}. \tag{6}$$

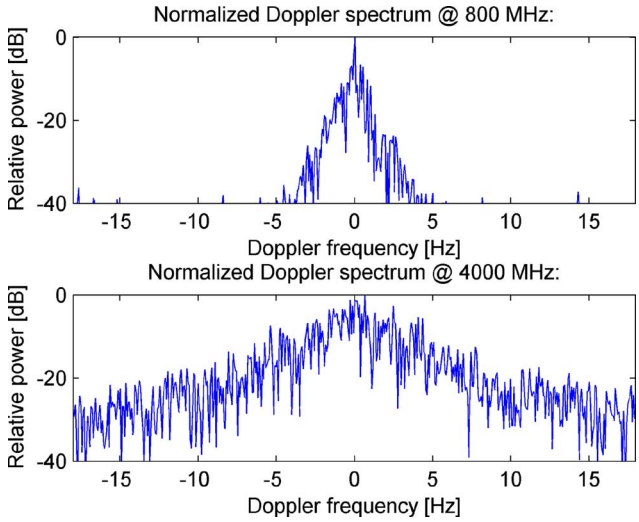

Fig. 2. Doppler power spectrum at two different frequencies obtained by (4). The RMS Doppler bandwidth for this set of data equal to 1.0 Hz at 800 MHz and 3.6 Hz at 4 GHz. Note that the RMD Doppler bandwidth can be 100 times larger with a 100 times faster mode-stirrer speed. However, the actual maximum speed of the mode-stirrer in the current SP RC is limited. In order to compare the Doppler spread using step-wise stirring to that using continuous stirring, we limit our "imaginary" speed for step-wise stationary stirring so that it takes 20 s for one revolution of the mode-stirrer. In the future, a separate faster stirring fan can be introduced so that much larger Doppler spread can be achieved with the same method studied in this letter.

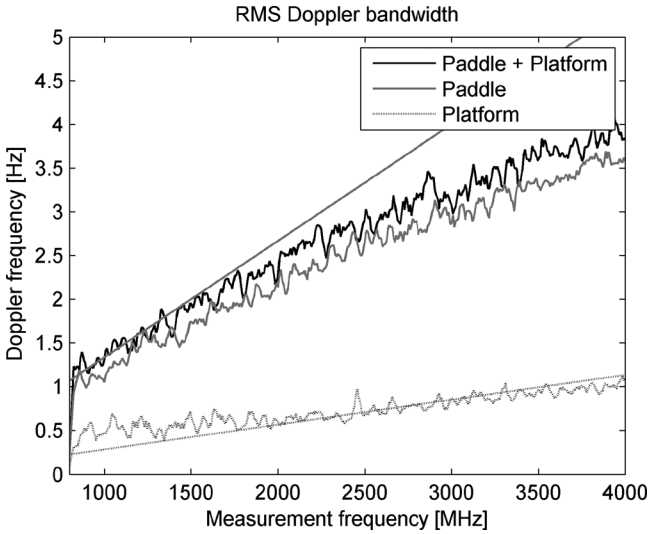

Fig. 3. RMS Doppler bandwidth for three different stirring sequences in RC computed by the stationary step-wise stirring approach. Straight lines are the theoretical maximum Doppler shift for a single-wave environment based on the maximum speed of the antenna on the platform (radius 27 cm), maximum radius of the stirrer (63 cm).

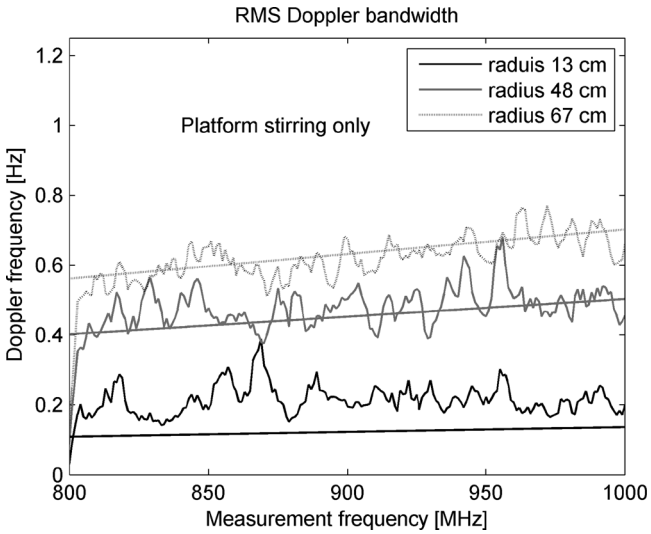

Fig. 4. RMS Doppler bandwidth measured in RC with step-wise stationary stirring for antenna located at different radii on the platform. Straight lines are maximum Doppler shift in a single-wave environment for the same platform cases, using (7).

The integrations in (6) should exclude noise floor (the level where Doppler spectrum becomes flat), which is around -40 dB. This agrees with [8]. This RMS Doppler bandwidth has been measured and calculated for the SP RC for three different stirring sequences: 1) only paddle; 2) only platform; 3) both paddle and platform. Total time for a revolution of each of the stirring sequences was 20 s. The results are shown in Fig. 3. Here, it can be concluded that, in this particular setup, the paddle is more efficient to generate Doppler than the platform, and that the combination is more efficient than each stirrer alone as expected.

To elucidate the overall picture, two theoretical Doppler shifts are added to Fig. 3 as well: one representing the platform and one representing the paddle. These are the theoretical maximum Doppler shifts available from the platform and paddle when a single wave is incident on each one of them from the worst possible angle of incidence. The maximum Doppler shift is from classical Doppler theory given by

$$f_{\mathrm{D}} = \frac{v}{\lambda} \tag{7}$$

where λ is the wavelength and v is the velocity. This is for our platform case given by $v = 2\pi r/T$, with T being the time for one platform rotation and r the radius of the position on the platform where DUT is located, i.e., the distance from the antenna to the platform center. The theoretical maximum Doppler shift curve for the platform in Fig. 3 is obtained by using $r = 27$ cm. Equation (7) can in principle also be used for the rotating paddle, with $r = 63$ cm being the maximum possible radius of it; see Fig. 4. However, for the paddle case, we need to multiply the right side of (7) by a factor of 2 because the rotating paddle reflects the waves like in a radar, so the Doppler shift is twice that of the Doppler observed due to a movement of either the receiver or transmitter in the same way as for a moving radar target. Such calculated "maximum" theoretical shifts are not expected to coincide with the actual measured ones in the RC because the waves in the RC perform multiple reflections between the walls of the chamber, so the same Doppler shifted wave may be shifted many times through multiple reflections from the same moving target (stirrer). They are still included in the graphs in order to relate the observed Doppler spread to the actual speed of the stirrers, and we see in Fig. 3 that such theoretical values and the RMS Doppler bandwidth actually follow each other quite well.

Two additional tests are performed to validate the method. The first validation is shown in Fig. 4. In this test, a 900-MHz dipole antenna is located on the platform at a radius r. Three

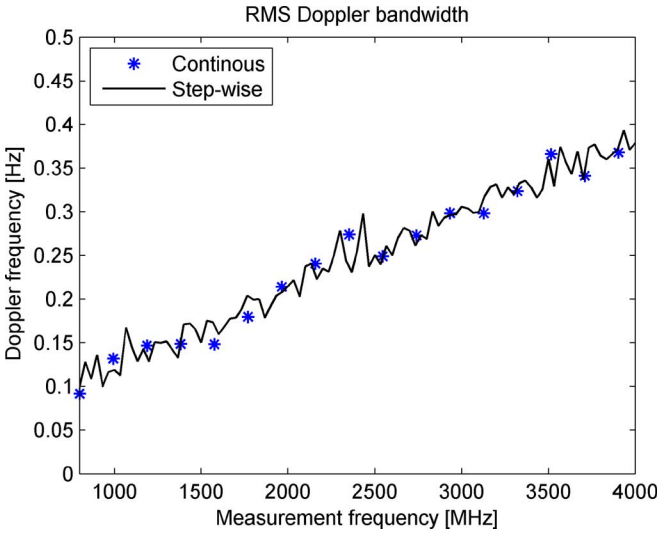

Fig. 5. Validation of RMS Doppler bandwidth obtained by using present step-wise stationary approach by comparison to results obtained from actual time-varying measurements using continuous movement of the stirrers with given speed at discrete frequencies.

measurements were performed with r equal to 13, 48, and 67 cm. The only things moving in the chamber during these measurements were the antenna on the platform and the cable connected to it. As can be seen in Fig. 4, the theoretical maximum Doppler shifts (7), with $T = 20$ s, are very close to the generated RMS Doppler shifts. The discrepancy for the smallest radius in Fig. 4 is believed to be due to the uncertainty of the actual DUT position. It should also be kept in mind that generated values are RMS values for the actual harsh multiple reflections environment in the RC, and theoretical values are maximum values for the single-wave case. As can be seen from (6), the RMS Doppler bandwidth is always smaller than the maximum Doppler shift in RC. They are proportional to each other. The proportionality factor depends on the shape of the Doppler spectrum. This means that the maximum Doppler shift with a certain speed in RC is larger than the corresponding Doppler shift in free space, which agrees with the claim in [10].

Second, the step-wise stationary method is validated with measurements during continuously moving stirrers by setting the VNA in continuous-wave mode at certain frequencies. In this case, the VNA was used to measure $S_{21}(f, t_n)$ 750 times, each of them for one complete rotation of the platform and paddle. The rotation time T was increased to 182 s in order to be able to capture the data with the data acquisition software, so the observed Doppler shift was very small; see Fig. 5. This figure shows good agreement between RMS Doppler bandwidths obtained by step-wise stationary and continuous measurements.

IV. Conclusion

We have demonstrated how Doppler power spectrum easily can be measured in an RC (or any controlled environment) during step-wise stationary stirring conditions, and how this can be used to determine the actual RMS Doppler bandwidth achieved during continuous stirring, which is the desirable mode of operation during OTA tests of active wireless stations. The approach has been validated over large bandwidth by comparison to results from time-domain Doppler measurements. The approach well illustrates the fact that fading speed determines Doppler spread in multipath environments, and that the Doppler spectrum scales linearly with stirring speed. The observed RMS Doppler bandwidth is similar in value to the theoretical maximum Doppler shift in a single-wave environment, which indicates that there exist excess or multiple Doppler shifted-wave components due to the multiple reflections in the chamber, although their effect is not very large.

References

[1] J. G. Kostas and B. Boverie, "Statistical model for a mode-stirred chamber," *IEEE Trans. Electromagn. Compat.*, vol. 33, no. 4, pp. 366–370, Nov. 1991.

[2] K. Rosengren and P.-S. Kildal, "Radiation efficiency, correlation, diversity gain and capacity of a six-monopole antenna array for a MIMO system: Theory, simulation and measurement in reverberation chamber," *IEE Proc. Microw. Antennas Propag.*, vol. 152, pp. 7–16, 2005.

[3] N. Serafimov, P.-S. Kildal, and T. Bolin, "Comparison between radiation efficiencies of phone antennas and radiated power of mobile phones measured in anechoic chambers and reverberation chamber," in *Proc. IEEE AP-S Int. Symp.*, San Antonio, TX, Jun. 2002, vol. 2, pp. 478–481.

[4] C. Orlenius, P.–S. Kildal, and G. Poilasne, "Measurement of total isotropic sensitivity and average fading sensitivity of CDMA phones in reverberation chamber," in *Proc. IEEE AP-S Int. Symp.*, Washington, DC, Jul. 3–8, 2005, vol. 1A, pp. 409–412.

[5] X. Chen, P.-S. Kildal, C. Orlenius, and J. Carlsson, "Channel sounding of loaded reverberation chamber for Over-the-Air testing of wireless devices – Coherence bandwidth and delay spread versus average mode bandwidth," *IEEE Antennas Wireless Propag. Lett.*, vol. 8, pp. 678–681, 2009.

[6] A. Goldsmith, *Wireless Communications*. Cambridge, U.K.: Cambridge Univ. Press, 2005.

[7] S. Stein, "Fading channel issues in system engineering," *IEEE J. Sel. Areas Commun.*, vol. SAC-5, no. 2, pp. 68–89, Feb. 1987.

[8] S. J. Howard and K. Pahlavan, "Doppler spread measurement of indoor radio channel," *Electron. Lett.*, vol. 26, no. 2, pp. 107–109, Jan. 1990.

[9] M. Souden, S. Affes, J. Benesty, and R. Bahroun, "Robust Doppler spread estimation in the presence of a residual carrier frequency offset," *IEEE Trans. Signal Process.*, vol. 57, no. 10, pp. 4148–4153, Oct. 2009.

[10] P. Hallbjörner and A. Rydberg, "Maximum Doppler frequency in reverberation chamber with continuously moving stirrer," in *Proc. Loughborough Antenna Propag. Conf.*, 2007, pp. 229–232.